Journal of ELECTRONIC MATERIALS, Vol. 47, No. 8, 2018
https://doi.org/10.1007/s11664-018-6338-y

Sensor Functionality of Conducting Polyaniline-Metal Oxide (TiO_2/SnO_2) Hybrid Materials Films toward Benzene and Toluene Vapors at Room Temperature

E. SUBRAMANIAN,[1,3] P. SANTHANAMARI,[1] and C. MURUGAN[1,2]

1.—Department of Chemistry, Manonmaniam Sundaranar University, Tirunelveli, Tamil Nadu 627012, India. 2.—Department of Chemistry, S. Veerasamy Chettiar College of Engineering and Technology, Puliangudi, Tamil Nadu 627 855, India. 3.—e-mail: esubram@yahoo.com

Polyaniline-metal oxide (TiO_2/SnO_2) organic–inorganic hybrid materials films were fabricated *in situ* on a printed circuit board (PCB) via drop coating technique. The mixture of aniline and metal oxide (TiO_2/SnO_2) dispersed in ethanol was applied along with an oxidant for the coating process. The formed material films were characterized by Fourier transform infra-red spectroscopy, x-ray diffraction and scanning electron microscopy techniques. The sensor functionality of the prepared films on PCB was investigated individually for the detection of benzene or toluene vapor at room temperature. The promptness of sensor response to analyte vapor and its recovery to air, as well as the concentration-dependent sensor functionality of the hybrid material films were investigated. The film form of hybrid materials has shown much improved sensor efficiency even at ambient air condition compared to the pellet form of the polyaniline-SnO_2 hybrid material reported earlier, which sensed the same analytes only in nitrogen atmosphere.

Key words: Polyaniline-SnO_2, polyaniline-TiO_2, hybrid materials, sensor functionality, benzene, toluene analytes

INTRODUCTION

Hydrocarbon and halogen-substituted organic solvents easily evaporate and pollute the indoor air at industrial sites and household regions. Most of these solvents and their vapors are hazardous and are known to cause diseases such as allergies, asthma, cancer and emphysema in human beings.[1] Thus, an awareness of the presence of these solvents vapors, their identification and estimation are very important from health and environmental points of view. Therefore, the development of sensor materials for the detection of benzene and related aromatic hydrocarbons such as toluene vapors has attracted much interest from researchers.[2–6]

Conducting polyaniline (PANI) has been reported for sensing of ammonia,[7] hydrocarbons[8] and chlorinated hydrocarbons.[9,10] But, the low efficiency and selectivity of pristine PANI limit its application as a sensor material. However, metal oxides such as TiO_2,[2] Y_2O_3,[3] WO_3[4] and SnO_2[11] have shown appreciable sensitivity toward benzene. They also show sensing functionality toward other chemical analytes. For instance, Au decorated SnO_2 nanoparticles show high response and selectivity towards ethanol.[12] Pd-doped SnO_2 based thick film array was applied for the detection of H_2, CH_4 and CO.[13] Nanostructured and nanocrystalline TiO_2-Cr_2O_3 mixed metal oxide was studied for the detection of NO_2.[14] Addition of SnO_2 is reported to enhance the gas sensing behavior of TiO_2 nanobelt.[15] However, these metal oxide sensors have an intrinsic drawback, i.e. they are operative only at higher temperature.[4,5,12–16]

Nevertheless, organic–inorganic hybrid composite (OIHC) materials involving metal oxides with the

(Received July 19, 2017; accepted April 26, 2018; published online May 21, 2018)

resultant synergic/complement property formed could overcome the shortcomings of metal oxide sensors.[17–20] Particularly, PANI-SnO_2 OIHC material is promising for supercapacitor,[21] optoelectronics[22] and ammonia gas-sensing.[20,23] The underlying principle for its prominence is the fact that PANI is a *p*-type semiconductor while SnO_2 is an *n*-type semiconductor, but their combination leads to newer properties with the formation of a p–n junction. Hence, PANI-SnO_2 hybrid material with inherent p–n heterojunctions and the associated electric field across such junctions can function as a better material in many respects than either pure PANI or pure SnO_2.[24,25] Using the phenomenon of p-n heterojunction formation from p-CuO and n-ZnO, highly sensitive thin film sensor for reducing gas H_2 has been reported.[26]

Carcinogenic benzene and related aromatic hydrocarbon solvent (e.g. Toluene) vapors have very weak interaction with the sensor materials and, therefore, studies on development of chemo-sensors for these vapors are limited. In our previous works[24,25] we developed chemo-sensors based on PANI-SnO_2 p–n junction hybrid materials and studied their sensing functionality in pellet form using a four-probe technique toward benzene/toluene analyte vapor. However, the sensor material, PANI-SnO_2 having high conductivity (0.7–3.3 S/cm) had affinity toward moisture in preference to the analyte molecules and thus N_2 atmosphere was necessary for their functionality. In other words, the PANI-SnO_2 chemo-sensor developed in our previous works could not be applied for sensing benzene/toluene vapor at air ambience. However, it has been our continuous interest to develop such sensors that are functionable at normal atmospheric condition. In order to attain this goal, in the present work we changed the method to prepare OIHC materials and also the sensor configuration (from pellet to film on a printed circuit board, i.e. PCB). Herein we report the sensor functionality of PANI-TiO_2/SnO_2 OIHC materials films developed *in situ* on PCB which work well even in air ambient condition.

EXPERIMENTAL PROCEDURE

Aniline (Merck) was purified by distillation over zinc dust. Ammonium peroxodisulfate (APS; Merck), SnO_2 (~ 325 mesh; Sigma-Aldrich), TiO_2 (99.8% anatase; Sigma-Aldrich) and other chemicals (Merck) were used without further purification. The printed circuit board, Cu wire, solder lead, etc. were purchased from a local market and conductive Ag paste from Eltecks Corporation, India. Water used in the preparation and washing was doubly distilled unless otherwise mentioned.

Synthesis of PANI and PANI-TiO_2/SnO_2 Hybrid Materials Films

A commercially available printed circuit board (PCB) was used as the substrate material for the *in situ* synthesis of sensor materials and for the sensor device fabrication mentioned next. It was a very cheap, easy to fabricate use-and-throw material. The large size PCB was cut into about 1 × 1 cm small square pieces. Two pre-polished copper wires functioning as two probes for the sensor experiments were inserted from the bottom of PCB through two adjacent holes (Fig. 1a), bent horizontally (like English letter U) and were then soldered to the PCB at two adjacent metal contact points of interlying distance 0.3 cm (3 mm) (Fig. 1b). The PCB with these two soldered contact points was used for the deposition of conducting polymer material as described next.

The synthesis was carried out by using *in situ* chemical oxidative polymerization method.[7] 0.1 M aniline in 0.2 M HCl taken in a micropipette (10–100μL finnpipete) was delivered 2 drops onto a watch glass. To this, 2 drops of APS in 0.2 M HCl were added and mixed well. Two drops of this mixed solution was then immediately dropped using a micropipette as a spot over the PCB and allowed to stand without any disturbance for about 1 h. Polymerization occurred and polyaniline was formed on the PCB as a thin layer. Conductive Ag paste was then applied only over the two soldering points on the PCB (and not on deposited sensor material) in order to have a good ohmic contact between the polymeric film and the copper-soldered points (Fig. 1b). Otherwise, the direct contact between polymer film and Cu wire was not ohmic because dilute HCl present in polymerization mixture slowly corroded the solder lead and an increase in resistance on every cycle of sensor experiment occurred across the contact; i.e., the resistance was not a constant parameter and consequently the ohmic behavior was not followed.

Five milligrams of TiO_2 was added to 1 mL of ethanol and was sonicated for about 15 min in order for the uniform dispersal of TiO_2 particles. Two

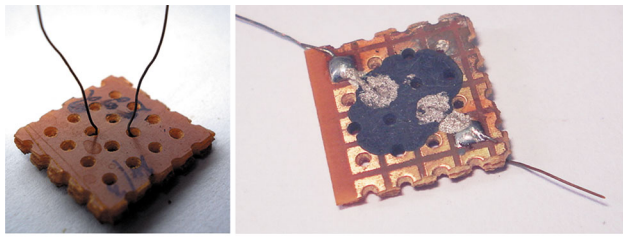

(a) (b)

Fig. 1. Photoimages of PCB (a) with copper wire insertion and (b) with complete sensor device fabrication.

drops of aniline, 2 drops of TiO_2-ethanol mixture and 2 drops of APS were taken in the watch glass using a micropipette and mixed well. Two drops of this mixture was then immediately dropped using a micropipette as a spot over the PCB as done for polyaniline. Polymerization occurred, and thus a polyaniline-TiO_2 composite film was formed *in situ* on the PCB. This is labeled as PANI-TiO_2. This procedure was repeated using SnO_2 in place of TiO_2 to prepare PANI-SnO_2 OIHC material film and is labeled as PANI-SnO_2. Electrical contact at the two adjacent Cu contact points (3 mm) was made using Ag paste.

Conductivity and Sensor Experiments

A sensor chamber of volume 900 mL was designed from glass vacuum desiccator with inlet and outlet for flow of gases. The sensor material film-coated PCB (PANI and PANI-TiO_2/SnO_2) with two Cu wire-Ag pasted probes and a solvent container were placed inside the chamber. The resistance of the PCB coated sensor material was measured at room temperature using a multimeter (MIC 16 H digital multimeter).

The sensor functionality of the PCB device with different sensor materials without/with vacuum (for 2 min) was monitored by measuring resistance change in the presence of analyte vapor for every 5 min and up to 30 min in a cycle. Three alternative response-recovery cycles of experiment for analyte vapor or air were done and for each cycle the resistance change at 5 min interval was measured. For each cycle, the sensor function/response was calculated in terms of normalized conductivity change % (NCC %) using Eq. 1.

$$\mathrm{NCC}(\%) = \frac{R_{\mathrm{Ana}} - R_{\mathrm{Air}}}{R_{\mathrm{Air}}} \times 100 \qquad (1)$$

where R_{Ana} = Resistance in analyte and R_{Air} = Resistance in air. NCC values (%) calculated for every 5 min time interval were averaged for all the three cycles and only the average NCC % values were computed and used for analyzing the sensor function. The different analyte concentrations in ppm were measured with a pre-calibrated gas chromatograph (Chemito, model 1000).

Characterization of the Samples

The prepared sensor materials were characterized using Fourier transform infrared spectroscopy (FTIR; JASCO 410), x-ray diffraction (XRD; PANalytical pro-MPG x-ray diffractometer) and scanning electron microscopy (SEM; Carl Zeiss EVO 18) techniques. XRD patterns of the samples (2θ = 10°–80°) were taken with a generator set at 30 kV and 30 mA at room temperature. All these characterizations were performed only for sensor materials removed from the PCB by slight scratching and not for any materials developed separately because only such characterizations will be correlatable to the actual operating condition of the materials.

RESULTS AND DISCUSSION

FTIR Characterization of the Samples

Figure 2 shows the FTIR spectra of pristine PANI, PANI-TiO_2 and PANI-SnO_2 hybrid materials. Pristine PANI exhibits weak peaks at 1615 cm^{-1}, 1492 cm^{-1}, 1302 cm^{-1} and 844 cm^{-1}. However, it exhibits intense peaks at 1399 cm^{-1}, 1204 cm^{-1}, 1157 cm^{-1}, 993 cm^{-1} and 662 cm^{-1}. The weak peaks are assignable to quinoid, benzenoid ring stretching, C-NH_2 amine and C-H out of plane bending vibrations.[23,24] respectively. The intense peaks are assigned to C = NH imine, C–H polaron, C–H in plane bending mode (conductivity peak), 1–4 disubstituted benzene ring and N–H bending mode,[27,28] respectively. Compared to previous reports,[27,28] herein all the IR peaks are observed at higher wavenumber positions. This may be due to the direct synthesis of material on PCB, non-washing of material (washing usually with acetone and acid) and presence of included water. In the case of PANI-TiO_2 hybrid material the TiO_2 peak[29] at 696 cm^{-1} appears only as a week peak (indicated by circle) and all the PANI peaks appear more or less at the same positions. The weaker peak at ~ 676 cm^{-1} (indicated by circle) in PANI-SnO_2 represents the presence of Sn-O-Sn vibration.[19] These observations confirm the formation of PANI and its metal oxide hybrid materials.

Structural Characterization of the Samples

Figure 3 displays the powder-XRD patterns of PANI and its hybrid materials. PANI exhibits broad signal at 24.88° indicating the presence of amorphous conducting form.[24] PANI-TiO_2 hybrid material exhibits sharp signals at several positions. The

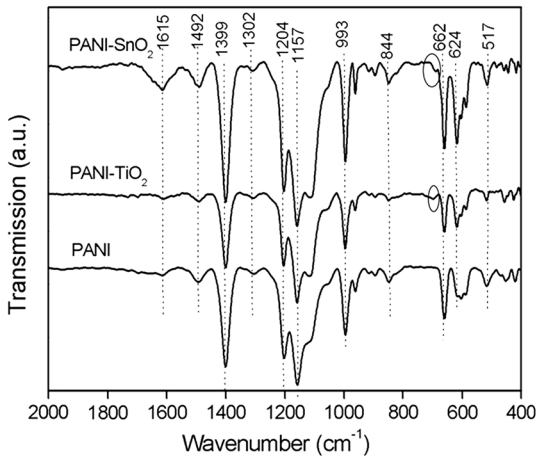

Fig. 2. FTIR spectra of PANI, PANI-TiO_2, and PANI-SnO_2 OIHC materials.

peaks corresponding to TiO_2 anatase structure (JCPDS file No. 89-4203) are found and indexed for corresponding hkl crystalline planes. For PANI-SnO_2 hybrid the peaks corresponding to SnO_2 are indexed and are matchable with the pattern in literature report (JCPDS file No. 78-1063). So observation of signals corresponding to PANI and TiO_2/SnO_2 for the hybrid materials indicates the hybrid material formation. Any XRD signal unassigned for PANI or its hybrid materials might have their origin on PCB material.

Figure 4 illustrates the SEM images of PANI and PANI metal oxide hybrid materials at lower and higher magnifications. PANI (a and b) has a mixed morphology of irregularly shaped amorphous material and spherical particles of submicron size. There is extensive agglomeration of PANI in the irregularly shaped particle region. In the case of PANI-TiO_2 hybrid material (c and d) similar morphology of PANI is observable; however, a large number of spherical particles of TiO_2 is also seen. These images also show the polymerization of aniline over TiO_2 particle and the resultant polyaniline coating/coverage over TiO_2 particles. For PANI-SnO_2 hybrid material also (e and f) the morphology is similar to that of PANI-TiO_2 hybrid. But a larger number of SnO_2 spherical particles is seen in the images. For this hybrid material PANI coating over SnO_2 is also clearly observable. All the three characterizations, FTIR, XRD and SEM confirm the PANI-metal oxide hybrid material formation.

Sensor Functionality of PANI and Its Hybrid Materials

With regard to the sensor functionality of the materials, the study was made on PANI, PANI-TiO_2 and PANI-SnO_2 OIHC materials films. All these materials films were exposed individually to the benzene or toluene solvent vapor for 30 min under the conditions of (a) without vacuum and (b) with vacuum. Without vacuum, the solvent evaporated under normal atmospheric pressure and the experimental condition was similar to the field condition. In category b with vacuum, the sensor chamber was evacuated for 2 min with suction pump and solvent evaporation was done under reduced atmospheric pressure. This condition caused faster and greater solvent evaporation and hence vapor concentration was higher.

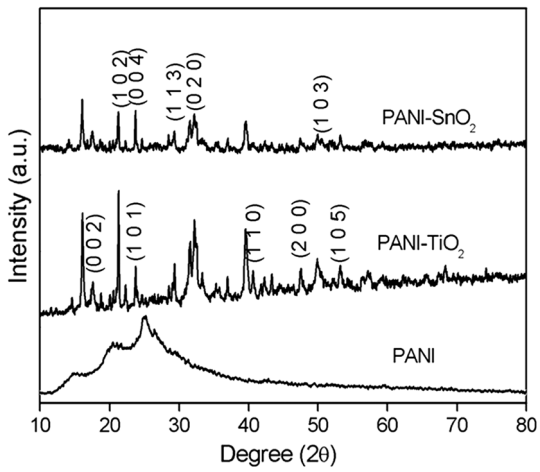

Fig. 3. XRD patterns of PANI, PANI-TiO_2, and PANI-SnO_2 OIHC materials.

Before the beginning of sensor experiment, the analyte vapor concentration was studied separately for 30 min evaporation for both a and b categories by measuring the analyte concentration with precalibrated GC. It was observed that the analyte vapor concentration was almost doubled under "with vacuum" category (b); benzene concentration change during 30 min without vacuum is 44 ppm to 144 ppm, while it is 129 ppm to 271 ppm with vacuum. Under similar condition toluene concentration change (29–76 ppm without vacuum and 67–131 ppm with vacuum) was lower than that of benzene. This is quite understandable because toluene has a higher boiling point (110.6°C) than benzene (80.1°C) and, therefore, toluene evaporation is slower than benzene. Concentration determination of solvent vapors was done in two separate experiments (in order to avoid any error) and only average values are given.

The primary data, namely the resistance of the sensor materials performed in three cycles of analyte and air are shown as the dynamic response-recovery profiles (Fig. 5). In these figures the two profiles at the bottom are for benzene and toluene analytes without vacuum, and the other two profiles at the top are for benzene and toluene vapors with vacuum.

A thorough examination of the data and the profiles gives the following inferences. All the materials are sensitive to analyte vapors and their change in concentration (without/with vacuum). As the concentration of the vapor is increased, the resistance of the materials is also increased. That means the materials show their response to higher analyte concentration by a decrease in conductivity. As the analyte vapor is removed by the introduction of air, the resistance of the materials gradually return to their original values. That means the conductivity of the materials is almost gained in air. The resistance/conductivity change of the three sensor materials (PANI, PANI-TiO_2 and PANI-SnO_2) is thus dynamic in first cycle. This sensor behavior is repeated in second and third cycles also. Altogether all the three materials show dynamic sensor response. Among the three materials, PANI-SnO_2 has the lower resistance in MΩ and exhibits clear sensor profiles.

From the primary resistance values the sensor functionality of the materials in terms of NCC % values were calculated. The sensor functionality profiles of the materials are shown in Figs. 6 and 7. A careful consideration of the profiles gives rise to

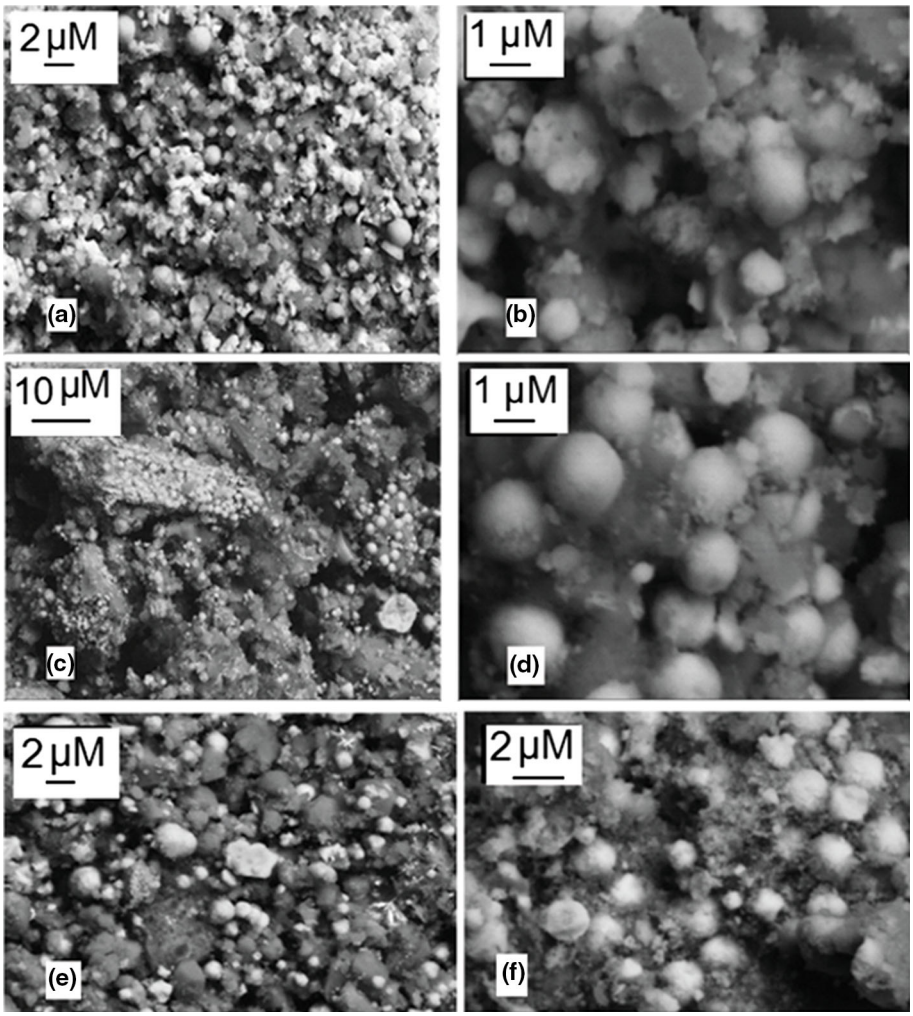

Fig. 4. SEM images of lower and higher magnifications of (a, b) PANI, (c, d) PANI-TiO_2, and (e, f) PANI-SnO_2.

certain inferences. Among the three materials PANI exhibits the lowest and PANI-SnO_2 exhibits the highest sensor functionality. The sensor functionality of all the materials is almost linear with respect to concentration of analyte. Comparing the profiles in Figs. 6a (benzene without vacuum) and 7a (benzene with vacuum), it is noticeable that sensor functionality of the sensor materials is doubled as the benzene concentration is also doubled. Comparison of the profiles in Figs. 6b (toluene without vacuum) and 7b (toluene with vacuum) also shows the enhancement in sensor response, i.e. NCC % with increase in toluene concentration. Comparison of sensor responses for benzene and toluene vapors at a given condition (without/with vacuum) leads to the observation that the materials show greater response for toluene than benzene. Although at a given condition the toluene vapor concentration is lower than that of benzene, the materials show greater sensor response only to toluene. This amazing observation clearly indicates that toluene analyte has greater level of interaction with sensor material than does benzene. Similar type of sensor observation has been made in our previous studies.[24,25] This greater sensor inducement from toluene is understandable by the fact that benzene has symmetrical structure and symmetrical π-electron cloud, whereas toluene has a methyl substituent at one carbon and thus its structure is unsymmetrical and the π-electron cloud is oriented towards the methyl substituent. This slight distortion in π-electron cloud and polarity may be responsible for the greater interaction of toluene with the sensor material.[30]

All the materials exhibit fast, reproducible and regenerative sensor responses with respect to benzene and toluene vapors at different concentrations. Dynamic response-recovery profiles shown in Fig. 5 have clearly established that the sensor response to analyte vapor is transient and momentary, as long as vapor is present in the sensor materials. As the vapor is replaced by air, the materials regain their resistance values. All these sensor observations and results give rise to the conclusion that the interaction between analyte vapor and sensor material is only of physical type (may be surface adsorption).

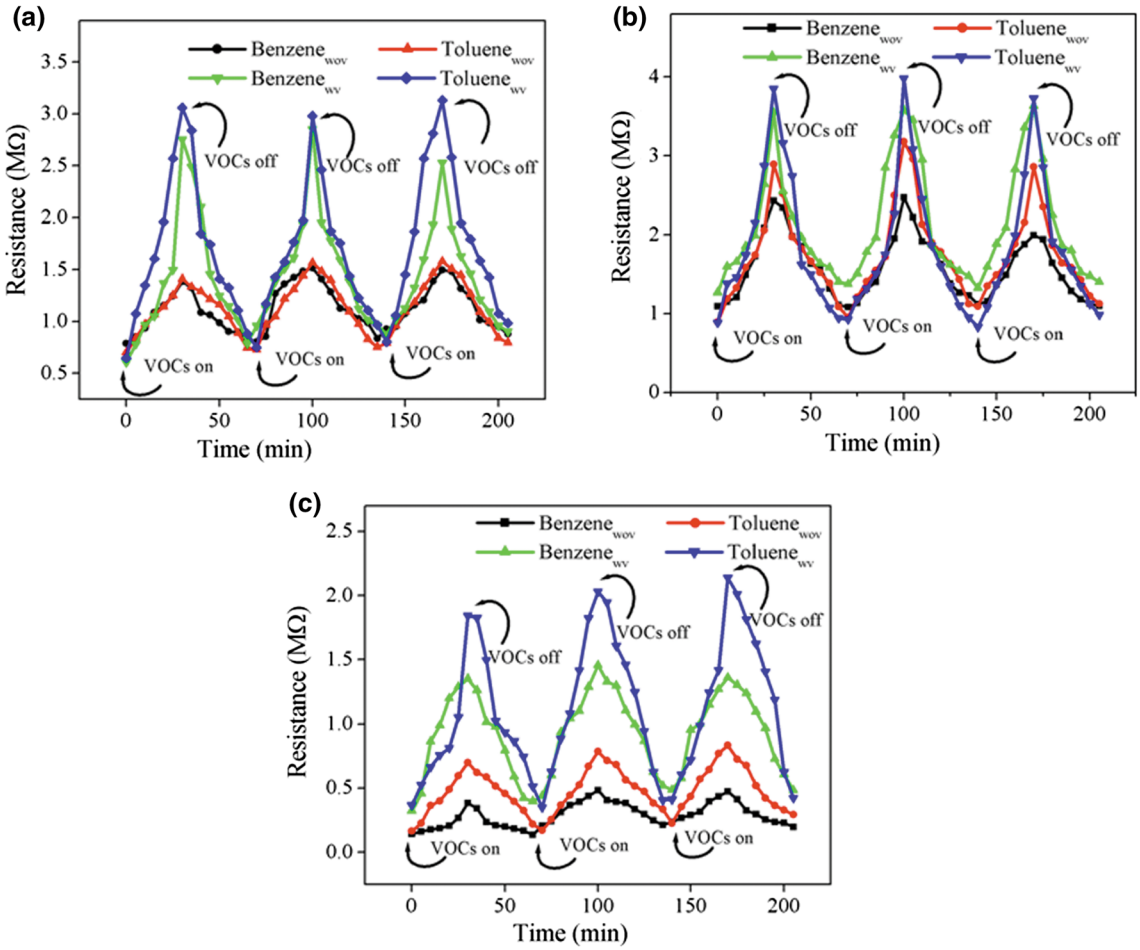

Fig. 5. Dynamic response-recovery profiles of (a) PANI, (b) PANI-TiO_2, and (c) PANI-SnO_2 toward benzene and toluene volatile organic compounds (VOCs); *wov* without vacuum and *wv* with vacuum.

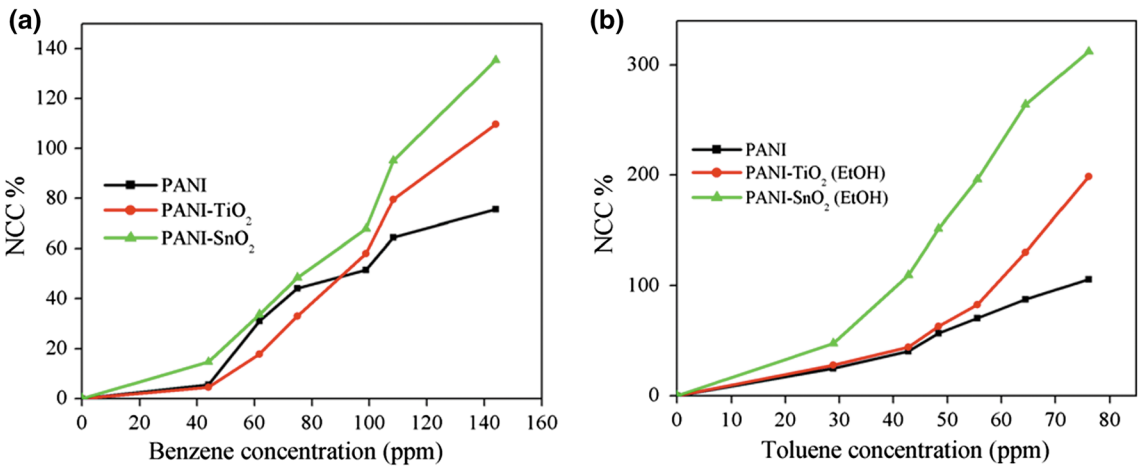

Fig. 6. Sensor functionality of the materils in (a) benzene and (b) toluene atmospheres without vacuum.

All the sensor responses have been observed and studied under normal atmospheric air only. This is an advantageous feature of the present materials, when one considers the sensor response of pellet form of PANI-SnO_2 hybrids observed only in N_2 atmosphere in our previous works.[24,25] The sensor response of present materials even at ambient air condition arises, perhaps, due to the involvement of at least a few facilitating factors such as (1) greater non-polar or hydrophobic nature of the hybrid

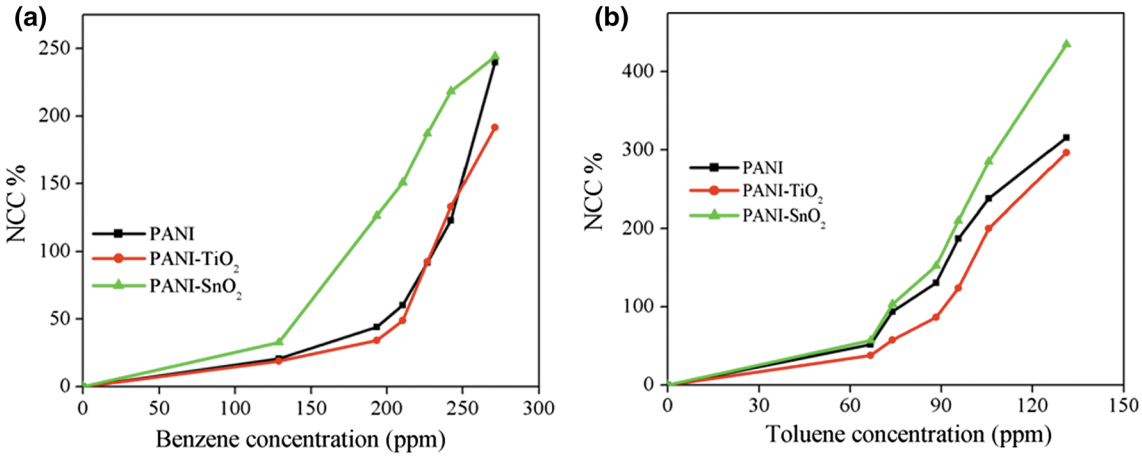

Fig. 7. Sensor functionality of the materils in (a) benzene and (b) toluene atmospheres with vacuum.

material film (so that moisture is repelled, evidence therefor is the high resistance in MΩ range for present materials compared to the high conductivity of 0.7–3.3 S/cm for previous work materials bearing hydrophilicity[31]), (2) transparent shiny surface of the film in contrast to the rough surface of the pellet, (3) continuity of material phase in film configuration compared to the discrete particles compact arrangement in pellet, (4) Ag paste ohmic contact (present work) rather than four-probe metal pin contact (previous work) etc.

Our results are compared with the previous literature reports. Polypyrrole has shown 2% sensitivity only with benzene and 7% with toluene at high concentration of 5000 ppm.[32] Metalloporphyrin functionalized single walled carbon nanotubes based field effect transistor has 30% sensitivity at 10 ppm benzene concentration.[33] The pellet form of PANI/SnO_2 could show, in our previous work, 16.93% sensitivity only with benzene and 19.53% with toluene at analyte concentration of 1650 ppm.[25] But the present results suggest that PANI-SnO_2 film formed on PCB exhibits the sensitivity (NCC %) of 130 at 140 ppm of benzene and 300 at 70 ppm of toluene. The highly promising sensor functionality of the present hybrid materials is definitely encouraging and is primarily due to the hydrophobic nature and film configuration of the present materials.

In order to have an insight into the sensor mechanism, the interaction between analyte vapor and the sensor material was studied by FTIR spectra of the solvent drop-added (via micropipette) sensor materials. During pellet preparation for FTIR analysis with spectral grade KBr, most of the added solvent evaporated and only the occluded and adsorbed vapor remained in the pellet. The FTIR spectra of fresh and vapor adsorbed sensor materials PANI and PANI-SnO_2 are shown in Fig. 8. A perusal of the spectra clearly suggests

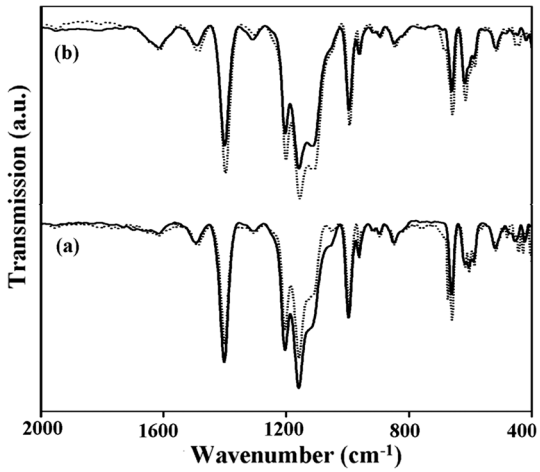

Fig. 8. FTIR spectra of fresh (solid line) and benzene vapor adsorbed (dotted line) (a) PANI and (b) PANI-SnO_2.

that there is an alteration in intensity (dotted line spectra) particularly in the peaks of imine and C–H in plane bending (conductivity peak) vibrations of PANI or PANI-SnO_2 on vapor association. Evidently these are the loci of interaction between sensor material and analyte. The analyte molecules may perturb the flow of π electrons of sensor material film, providing friction/resistance and thereby they decrease the film conductivity.[25,31] Extent of perturbation is manifested as sensor functionality and is read out as NCC % values. Further, there is consistence between sensor functionality of the materials and the degree of FTIR spectral changes. Greater the sensor function greater is the spectral change. For example, benzene with corresponding sensor inducement produces larger spectral shifts in PANI-SnO_2 (efficient sensor) in comparison to PANI (moderate sensor). Thus, IR spectral observation substantiates the sensor functionality.

CONCLUSIONS

All the sensor materials developed in the present work produce sensor responses and their behaviors are sensitive to change in concentration of the analyte vapor and change in the chemical nature of the vapor (benzene/toluene). The sensor functionality of all the materials has been observed under normal atmospheric condition, even in the presence of atmospheric moisture, which is an advantageous feature of the present materials. The sensor materials developed and deposited on PCB are in the milligram scale ($\sim$ 2 mg) while the analyte vapor benzene and toluene are introduced in the microscale level (ppm). Therefore, the present work represents the development of milliscale sensor materials for microscale analyte vapors. The PCB used in the present work is very cheap (maybe $<$ 1.0 Indian Rupee) and the cost involved in mg level of sensor material is very low. Therefore, it can be said that the present work has developed use-and-throw sensor devices for carcinogenic benzene and toluene vapors functionable at room temperature.

REFERENCES

1. T. Godish, *Air Quality*, 2nd ed. (Chelsea, MI: Lewis Publishers, 1991), p. 339.
2. M. Mabrook and P. Hawkins, *Sens. Actuators B* 75, 195 (2001).
3. Z. Rao, L. Liu, J. Xie, and Y. Zeng, *Luminescence* 23, 163 (2008).
4. M. Ke, M. Lee, C. Lee, and L. Fu, *Sensors* 9, 2895 (2009).
5. R. Leghrib, A. Felten, F. Demoisson, F. Reniers, J.-J. Pireaux, and E. Llobet, *Carbon* 48, 3477 (2010).
6. B. Ghaddab, F. Berger, J.B. Sanchez, P. Menini, C. Mavon, P. Yoboue, and V. Potin, *Sens. Actuators B* 152, 68 (2011).
7. P.P. Sengupta, S. Barik, and B. Adhikari, *Manufact. Proc.* 21, 263 (2006).
8. J.G. Roh, H.R. Hwang, J.B. Yu, J.O. Lim, and J.S. Huh, *J. Macromol. Sci. A* 39A, 1095 (2002).
9. G. Anitha and E. Subramanian, *Sens. Actuators B* 92, 49 (2003).
10. G. Anitha and E. Subramanian, *Sens. Actuators B* 107, 605 (2005).
11. A.K. Srivastava, *Sens. Actuators B* 96, 24 (2003).
12. Y. Li, F.-X. Zhao, X.-X. Lian, Y.-L. Zou, Q. Wang, and Q.-J. Zhou, *J. Electronic Mater.* 45, 3149 (2016).
13. M. Choudhary, V.N. Mishra, and R. Dwivedi, *J. Electron. Mater.* 42, 2793 (2013).
14. M.R. Mohammadi and D.J. Fray, *J. Electron. Mater.* 43, 3922 (2014).
15. W. Zeng, T. Liu, and Z. Wang, *J. Mater. Chem.* 22, 3544 (2012).
16. D. Lee, J. Jung, J. Lim, J. Huh, and D. Lee, *Sens. Actuators B* 77, 228 (2001).
17. L. Geng, Y. Zhao, X. Huang, S. Wang, S. Zhang, and S. Wu, *Sens. Actuators B* 120, 568 (2007).
18. L. Geng, *Trans. Nonferrous Met. Soc. China* 19, s678 (2009).
19. J. Zhang, S. Wang, M. Xu, Y. Wang, H. Xia, S. Zhang, X. Guo, and S. Wu, *J. Phys. Chem. C* 113, 1662 (2009).
20. H. Tai, Y. Jiang, G. Xie, and J. Yu, *J. Mater. Sci. Technol.* 26, 605 (2010).
21. Z. Hu, Y. Xie, Y. Wang, L. Mo, Y. Yang, and Z. Zhang, *Mater. Chem. Phys.* 114, 990 (2009).
22. K. Dutta and S.K. De, *Mater. Lett.* 61, 4967 (2007).
23. N.G. Deshpande, Y.G. Gudage, R. Sharma, J.C. Vyas, J.B. Kim, and Y.P. Lee, *Sens. Actuators B* 138, 76 (2009).
24. C. Murugan, E. Subramanian, and D.P. Padiyan, *Syn. Met.* 192, 106 (2014).
25. C. Murugan, E. Subramanian, and D.P. Padiyan, *Sens. Actuators B* 205, 74 (2014).
26. S. Mridha and D. Basak, *Semicond. Sci. Technol.* 21, 928 (2006).
27. E. Subramanian, G. Anitha, and N. Vijayakumar, *J. Appl. Polym.* 106, 673 (2007).
28. M. Reka Devi, B. Lawrence, N. Prithvikumaran, and N. Jayakumaran, *Int. J. Chemtech. Res.* 6, 5400 (2014).
29. H. Nur, L.I. Misnon, and L. Khengwei, *Int. J. Photoenergy* 98548, 1 (2007).
30. M.D. Imisides, R. Jhon, and G.G. Wallace, *ChemTech* 26, 19 (1996).
31. E. Subramanian, B. Mercy Leela Jeyarani, C. Murugan, and D. Pathinettam Padiyan, *J. Chem. Mater. Res.* 5, 129 (2016).
32. H.R. Hwang, J.G. Roh, D.D. Lee, J.O. Lim, and J.S. Huh, *Met. Mater. Int.* 9, 287 (2003).
33. A.D. Rushi, K.P. Datta, P.S. Ghosh, A. Mulchandani, and M.D. Shirsat, *J. Phys. Chem. C* 118, 24034 (2014).